THE JOURNAL OF PROSTHETIC DENTISTRY

CLINICAL RESEARCH

Three-dimensional in vivo and finite element analyses of peri-implant bone remodeling after superstructure placement

Itt Assoratgoon, DDS,[a] Boyang Wan, BE, ME, PhD,[b] Taichi Tenkumo, DDS, PhD,[c] Tomoya Sato, DDS, PhD,[d] Tetsuo Kawata, DDS, PhD,[e] Ramadhan Hardani Putra, DDS, MDSc, PhD,[f] Chi Wu, BE, ME, PhD,[g] Hiroshi Egusa, DDS, PhD,[h] Qing Li, BE, ME, PhD,[i] Keiichi Sasaki, DDS, PhD,[j] and Yoda Nobuhiro, DDS, PhD[k]

ABSTRACT

Statement of problem. Understanding the factors affecting loading-induced longitudinal peri-implant bone changes is crucial for successful implant-supported prosthetic treatment.

Purpose. The purpose of the study was to assess the biomechanical factors influencing 3-dimensional changes in the peri-implant bone volume and buccal bone thickness (BBT) with follow-up cone beam computed tomography (CBCT) images and finite element analysis (FEA).

Material and methods. Twelve study participants received dental implants without bone augmentation, resulting in the evaluation of 22 posterior dental implants. Each participant underwent 3 separate CBCT scans: the first at 3 months after loading, followed by scans at 15 months and 27 months after loading. CBCT images were superimposed at each interval with an image-processing software program. The peri-implant buccal bone area was determined as the volume of interest (VOI), and volumetric change in VOI and changes in BBT at 2, 4, and 6 mm below the implant platform were measured. FEA was performed to examine the mechanical stimulation in the VOI with occlusal force data obtained from the Dental Prescale. Interobserver reliability was evaluated by 3 experienced prosthodontists and dentists experienced with dental implants. Linear regression analyses were performed to evaluate the relationship between variables.

Results. Occlusal force and mechanical stimulation (strain energy density [SED]) in the VOI demonstrated a positive correlation; moreover, a positive correlation was observed between SED and bone volume loss in the VOI at 3 and 27months after loading. Similar correlations were observed with BBT, except at a depth of 6 mm under the implant platform. The interclass correlation coefficient values were 0.995 for volume and 0.982 for BBT, thereby indicating a high level of agreement among the observers' measurements.

Conclusions. This combined FEA and clinical study suggested that force-induced bone remodeling depends on the occlusal force in the early phases after superstructure placement. (J Prosthet Dent 2025;133:1535-1544)

Long-term peri-implant bone preservation is an important indicator of successful implant-supported prostheses.[1] Those provided under current evidence-based clinical procedures can result in the long-term preservation of healthy peri-implant bone tissue.[2,3] Nevertheless, peri-implant bone resorption or loss of osseointegration can occur even after prosthetic treatment, which has been attributed to peri-implantitis for

Supported by KAKENHI through the Japan Society for the Promotion of Science (JSPS) (grant no. JP19K10198; grant no. 20K18623), Japan.
The authors declare that they have no known competing financial interests or personal relationships that could have appeared to influence the work reported in this paper.
[a]Graduate student, Division of Advanced Prosthetic Dentistry, Tohoku University Graduate School of Dentistry, Miyagi, Japan.
[b]Postdoctoral Researcher, School of Aerospace, Mechanical and Mechatronic Engineering, The University of Sydney, Sydney, Australia.
[c]Lecturer, Division of Advanced Prosthetic Dentistry, Tohoku University Graduate School of Dentistry, Miyagi, Japan.
[d]Research Assistant, Division of Advanced Prosthetic Dentistry, Tohoku University Graduate School of Dentistry, Miyagi, Japan.
[e]Research Assistant, Division of Advanced Prosthetic Dentistry, Tohoku University Graduate School of Dentistry, Miyagi, Japan.
[f]Assistant Professor, Department of Dentomaxillofacial Radiology, Faculty of Dental Medicine, Universitas Airlangga, Surabaya, Indonesia.
[g]Postdoctoral Researcher, School of Aerospace, Mechanical and Mechatronic Engineering, The University of Sydney, Sydney, Australia.
[h]Professor, Division of Molecular and Regenerative Prosthodontics Tohoku University Graduate School of Dentistry, Japan.
[i]Professor, School of Aerospace, Mechanical and Mechatronic Engineering, The University of Sydney, Sydney, Australia.
[j]Professor, Laboratory for Redox Regulation, Tohoku University Graduate School of Dentistry, Miyagi, Japan.
[k]Professor, Division of Advanced Prosthetic Dentistry, Tohoku University Graduate School of Dentistry, Miyagi, Japan.

Clinical Implications

This research showed that by combining FEA technology and individual patient data, a visual and calculable evaluation could be made. Moreover, the results suggested that the importance of loading in the first year after superstructure placement should be emphasized, as it is the period with the greatest effect on bone remodeling associated with force.

various biological and mechanical reasons.[4–7] To avoid such complications and ensure successful long-term treatment outcomes, understanding the pathology of peri-implantitis and the mechanobiological response of peri-implant bone is critical.

Computed tomography (CT) and histomorphological image analyses have been used for investigating peri-implant bone healing and remodeling processes.[8] Histomorphological images can provide detailed information on the bone remodeling condition. However, the use of histomorphological analyses has been limited only to animals, and its clinical application in humans is challenging.[9] Although cone beam CT (CBCT) has been widely used for alveolar bone assessment during treatment planning and peri-implant bone evaluation after placement, CBCT images alone do not provide researchers with the necessary level of detailed mechanobiological information.[10] Thus, experiments using computer-aided engineering techniques, such as finite element analysis (FEA), offer a valuable avenue for addressing the issues concerning the study of bone remodeling in humans.[10] FEA allows for the simulation of intricate interactions among oral structures, prostheses, and implants, thereby facilitating a comprehensive investigation of the interdependencies among relevant factors, the challenges notwithstanding.[11,12] However, FEA has certain inherent limitations, including conveying inaccurate bone morphology, boundary conditions, and material properties, which can significantly affect the outcome of the experiment.[13–15] Despite variations in bone morphology among patients, many FEA studies tend to use bone models that are specifically created for the experiment.[16–18] Efforts have been made to simulate the natural conditions of the bone and oral environment by constructing an FEA model with CBCT images of actual patients. This approach provides a more precise representation of an individual's specific condition.[19–22] In addition, certain studies have incorporated the measurement of participants' occlusal force as input data to enable a more accurate FEA.[23]

As peri-implant bone changes in the buccal area are notably more pronounced than in other regions,[24,25] the present study examined biomechanical factors influencing longitudinal alterations in the peri-implant buccal bone area after superstructure placement by using the clinical data of actual patients who received fixed implant-supported prosthetic treatment. The null hypothesis was that loading forces after superstructure placement would have no impact on peri-implant bone remodeling.

MATERIAL AND METHODS

The research protocol for this study was approved by the Research Ethics Committee of Tohoku University Hospital (2018–2-203–1). Participants provided with implant-supported prostheses at Tohoku University Hospital were included in this study. Participants were informed about the purpose of the study and asked to sign the informed consent forms. The inclusion and exclusion criteria of the participants are listed in Table 1.

A software program (SimPlant; Materialise Dental) was used for 3D surgical planning for the implant location, and a standard tessellation language (STL) surgical guide (SurgiGuide; Materialise Dental) was used for the implant placement surgery. All the implants (Straumann Standard Plus RN; Institut Straumann AG) were placed by using a single-stage method, and the insertion torque value of all the implants was over 35 Ncm. For all implants, interim restorations were used for 3 months before the definitive restoration was placed. After the definitive restoration, the participant was followed up approximately every 4 months for prosthetic and oral hygiene examinations.

Three separate CBCT scans (3D Accuitomo; MORITA Corp.) were performed for each participant as follows: 3 months after interim restoration placement (at definitive restoration placement) (3 M), 15 months (15 M), and 27 months loading (27 M). The exposure settings were 90 kV and 35 mA, and the scanning parameters were voxel size, 0.225 mm; field of view, 14×8 cm; and slice thickness 0.25 mm.

A system (Dental Prescale; GC) was used to measure the occlusal force applied to each implant in maximum intercuspal position with maximum voluntary clenching.[25] The digital imaging and communications in medicine (DICOM) data of each CBCT scan was

Table 1. Participant inclusion and exclusion criteria

Inclusion Criteria	Exclusion Criteria
Is over 20 years old	Has peri-implantitis
Has one or more teeth missing, replaced with an implant-supported prosthesis	Has more than four consecutive missing teeth
Has no uncontrolled systemic disease	Has a history of head and neck radiotherapy
Implant is placed after a minimum healing period of four months	Has severe parafunctional habits
	Is pregnant or has potential for pregnancy
	Lacks sufficient capacity to make decisions

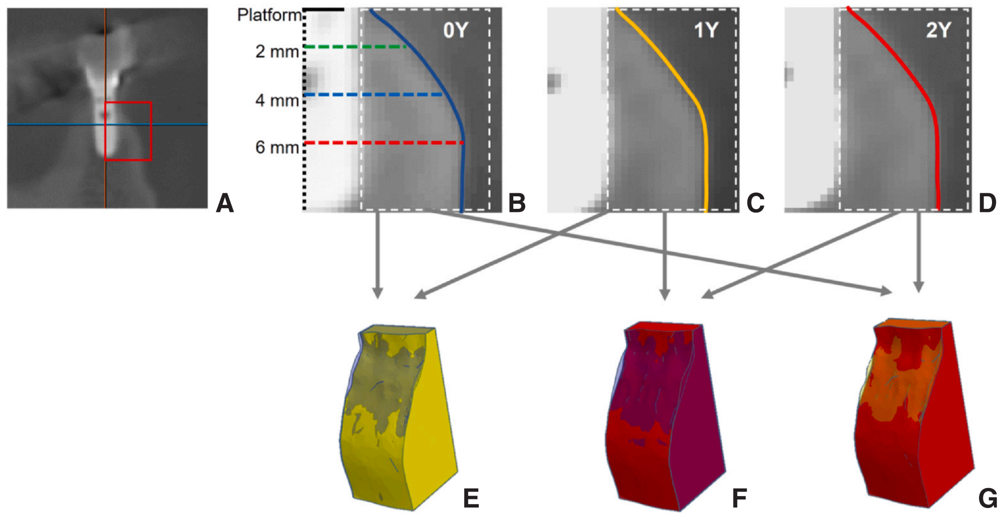

Figure 1. Methods for measuring time-dependent buccal bone volume and thickness changes. A, Reformat of cone beam computed tomography (CBCT) images. *Red box* represents volume of interest for bone volumetric changes. B, CBCT made 3 months after loading. *Blue line* shows example of buccal bone outer surface drawing. *Colored dotted lines* show measurement position (distance from implant platform) of buccal bone thickness. C, CBCT made 15 months after loading. D, CBCT made 27 months after loading. E-G, Examples of superimposition of 3-dimensional buccal bone area (E: 3–15M, F: 15–27M, G: 3–27M). M, months after loading.

processed with an image processing software program (ScanIP; Simpleware) to generate a 3D digital model of each image. Anatomic landmarks such as the mental foramen or incisive foramen and the implant body served as reference geometries for the superimposition of the CBCT images made at different times. The implant body and the peri-implant buccal bone were isolated, forming the volume of interest (VOI). This extended vertically from the implant platform to the implant apex and horizontally from the lingual border of the implant body to the outer surface of the most convex buccal bone (Fig. 1A). Additionally, the VOI encompassed 2 mm on the mesial and distal sides of the implant. The surface profile of the buccal bone was defined by pixel intensity (grayscale), which was determined by setting the intensity threshold and manual adjustment by filling and deleting each CBCT image slice outlining the buccal bone surface layer-by-layer, thereby enabling the investigation of the volume in the same region at different time points (Fig. 1B-D). The models were subsequently superimposed based on the implant body to measure the volume changes between 3 M and 15 M, 3 M and 27 M, and 15 M and 27 M (Fig. 1E-G). Buccal bone thickness (BBT) was also measured as the distance from the implant surface at the mesiodistal center of the implant body to the outer surface of the buccal bone on the cross-sectional image placed perpendicular to the teeth arch by the SimPlant. The BBT was measured at 2, 4, and 6 mm below the implant platform from the implant axis at 3 different times (3 M, 15 M, and 27 M)[26] (Fig. 1B). To ensure the reliability of the measurements for both volume and BBT, interobserver reliability was evaluated by 3 prosthodontists experienced with dental implants (N.Y., I.A., T.S.). The intraclass correlation coefficient (ICC) and typical error of measurement (TEM) were calculated to assess the agreement among the 3 observers.[27]

FEA was performed individually on all subjected implants. The STL files of the implant body and abutment were created based on µCT scans (ScanXmate-E090; Comscan) to ensure a precise definition of the 3D geometric model. The STL files of the superstructure shape were created by scanning each participant intraorally with an intraoral scanner (TRIOS 3; 3Shape A/S). Based on the CBCT images obtained after superstructure placement, jawbone geometric models were created for each participant (Fig. 2). The cortical and cancellous bones were separated based on the grayscale values with the image processing software program (ScanIP; Simpleware). Surface refinement was conducted to remove spike-like artifacts. The 3D geometric data of the implant components and superstructure correlated with the position on the CBCT images during model assembly. The models were then cropped to make a partial jawbone model including the implant and surrounding bone. The boundary condition was provided on both the mesial and distal sectional surfaces of the partial jawbone model. It was assumed that complete osseointegration had occurred at the implant–bone interface. The implant components, including the implant body, abutment, and superstructure, were also assumed to be perfectly bonded.[28]

The FEAs were performed with a software program (ABAQUS; Dassault Systems). The FE models were meshed with 4-node linear tetrahedron elements (C3D4). A mesh convergence test was performed to

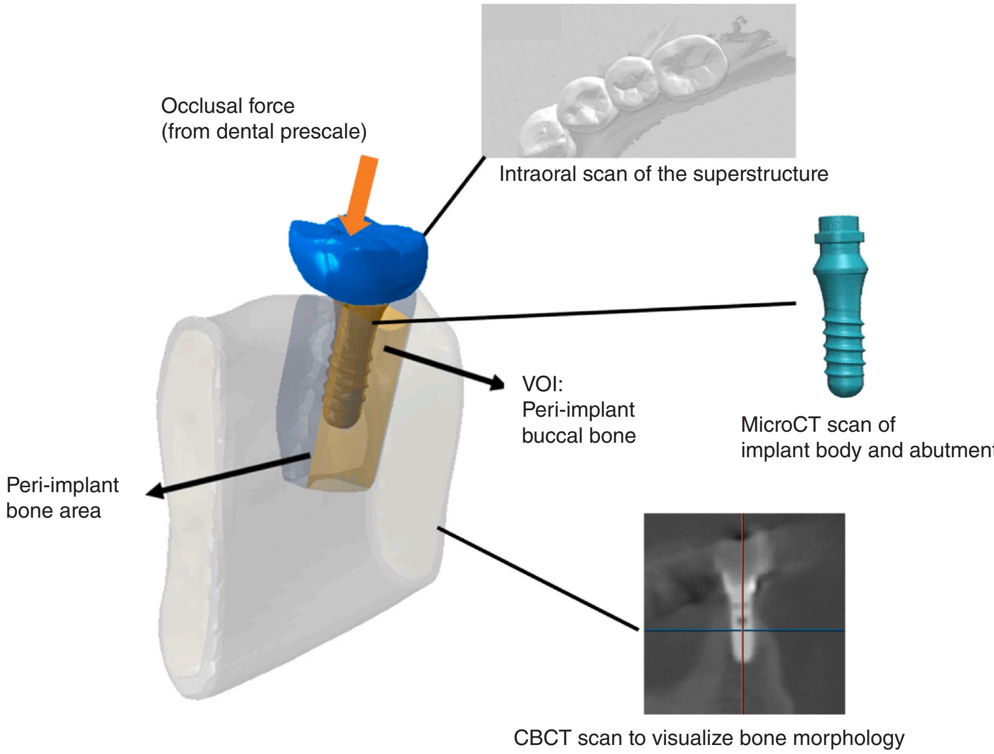

Figure 2. Components of finite element model assembly. CBCT, cone beam computed tomography.

determine the appropriate mesh size for the models by balancing computational accuracy and cost.[29] According to the convergence test, the global mesh size was 0.5 mm for the entire model; consequently, the corresponding number of elements was 290 096 (degrees of freedom: 159 360) on average. The implant, crown, and alveolar bone were considered homogenous, isotropic, and linear elastic materials for the FEA. The required material properties were obtained from the existing literature (Table 2).[30] Strain energy density (SED) was used as the mechanical stimulus in the jawbone, which has been reported to play an important role in regulating the bone remodeling process.[31,32]

The occlusal force obtained from the Dental Prescale was considered the magnitude of the input force on the superstructure in the FEA. The location of loading was determined only at the point on the superstructure where the maximum load was applied to simplify the analysis (Fig. 2). Moreover, the loading angulation was set as perpendicular to the point. In participants with a splinted superstructure, the occlusal force obtained from the Dental Prescale on each superstructure was regarded as the load exerted on each implant.[33]

The relationship between the occlusal force as an independent variable and SED in the VOI measured by FEA as the dependent variable was evaluated with the R^2 value. The relationships among SED as an independent variable and bone volume and BBT changes as dependent variables were evaluated with R^2 (α=.01). Statistical analyses were performed with a software program (JMP Pro 17; JMP Statistical Discovery LLC).

Table 2. Material properties used in finite element analysis

Material	Young Modulus (GPa)	Poisson Ratio
Titanium implants	110	0.3
Zirconia crown	200	0.27
Cortical bone	18	0.3
Cancellous bone	1	0.3

RESULTS

Twenty-two implants from 12 participants were studied. Although the recommended sample size was 25 based on the power analysis for linear regression analysis performed with a power level of 0.80, 3 dropouts during the follow-up period reduced the sample size to 22, which may decrease the generalizability of the study. Nevertheless, the analysis was performed to gain preliminary insights despite this limitation. Table 3 shows the participant demographics and implant properties. The participants included 7 women and 5 men, with ages ranging from 53 to 77 years. The mean occlusal force measured on a single implant was 96.1 N, with a maximum force of 200 N and a minimum force of 20 N.

The measurements of volume and BBT were calibrated. The computed ICC values were 0.995 for volume

Table 3. Participant demographic data

Implant No.	Participant	Age (Years)	Type of Superstructure	Location	Length (mm)	Diameter (mm)	Loading Force (N)
1	1	63	Non-Splinted	44	10	4.1	75
2	2	77	Non-Splinted	35	10	4.1	40
3	3	66	Non-Splinted	14	10	4.1	40
4	4	72	Splinted	35	10	3.3	50
5			Splinted	44	10	4.1	55
6	5	75	Splinted	34	10	4.1	40
7			Splinted	44	10	4.1	20
8	2	77	Non-Splinted	36	10	4.8	200
9	6	65	Non-Splinted	36	10	4.1	175
10	7	53	Non-Splinted	37	10	4.8	200
11	8	68	Non-Splinted	46	10	4.1	90
12	9	54	Non-Splinted	36	8	4.1	70
13	10	64	Non-Splinted	27	8	4.8	200
14	4	72	Splinted	36	10	4.1	70
15			Splinted	37	10	4.1	100
16			Splinted	46	10	4.1	190
17	5	75	Splinted	36	8	4.8	60
18			Splinted	46	10	4.1	20
19	11	64	Splinted	16	10	4.1	70
20			Splinted	17	10	4.1	70
21	12	77	Splinted	46	8	4.8	140
22			Splinted	47	8	4.8	140

and 0.982 for BBT, thereby indicating a high level of agreement among the observers' measurements. The TEM values were 0.14 mm for BBT and 5.08 mm^3 for the volume in the VOI, suggesting a strong consistency in their assessment. These findings imply that the measurements made by the 3 observers were reliable and could be used in further analyses.

Alterations in the bone volume at specified intervals (3 M to 15 M, 15 M to 27 M, 3 M to 27 M) were precisely measured (Fig. 3). Notably, the changes observed during 3–15M were significantly more pronounced than those during 15–27M. The independent 2-sample *t* test was performed with the assumption of normal distribution using the Shapiro–Wilk test ($P<.01$), resulting in a subtle difference between 3–15M and 3–27M. Additionally, volume loss was significantly more prominent in the molar (mean: 5.2 mm^3, standard deviation [SD]: 1.98 mm^3) than in the premolar clinical scenarios (mean: 1.81 mm^3, SD: 1.38 mm^3) ($P<.01$).

Time-dependent BBT changes were measured at 3 different depths in each period (Fig. 4A-C). The change in BBT during 3–27M was significantly different from the change during 3–15M at all 3 depths ($P<.01$). The majority of the BBT alterations might occur during the initial year after definitive restoration placement. Figure 4B shows the occurrence of minimal changes after 15 M, with negligible changes in some clinical scenarios.

For all the implants, the maximum SED was concentrated around the neck of the implant in the cortical bone area, especially at the contact area between the peri-implant bone and implant (Fig. 5). Figure 6 shows a significant positive relationship between the loading force and average SED in the peri-implant buccal bone area ($R^2=.31$, $P<.01$).

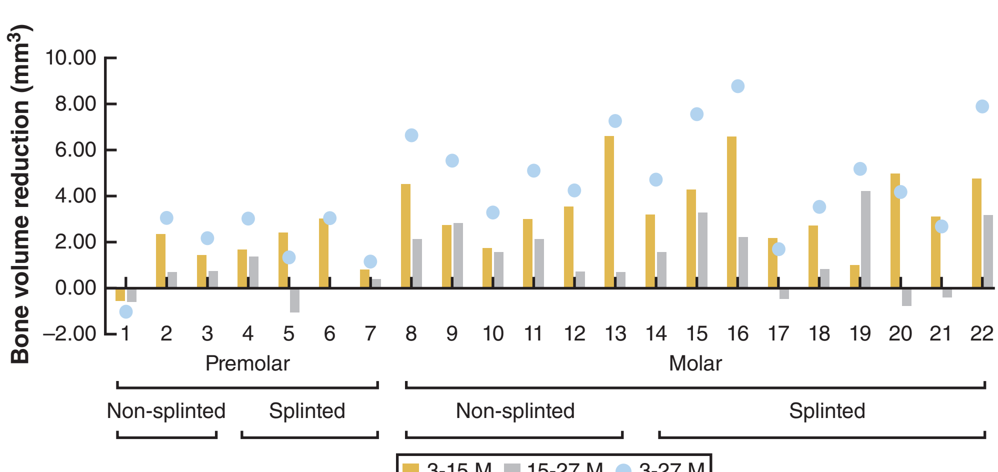

Figure 3. Buccal bone volume loss at different time intervals (3–15M, 15–27M, 3–27M). M, months after loading.

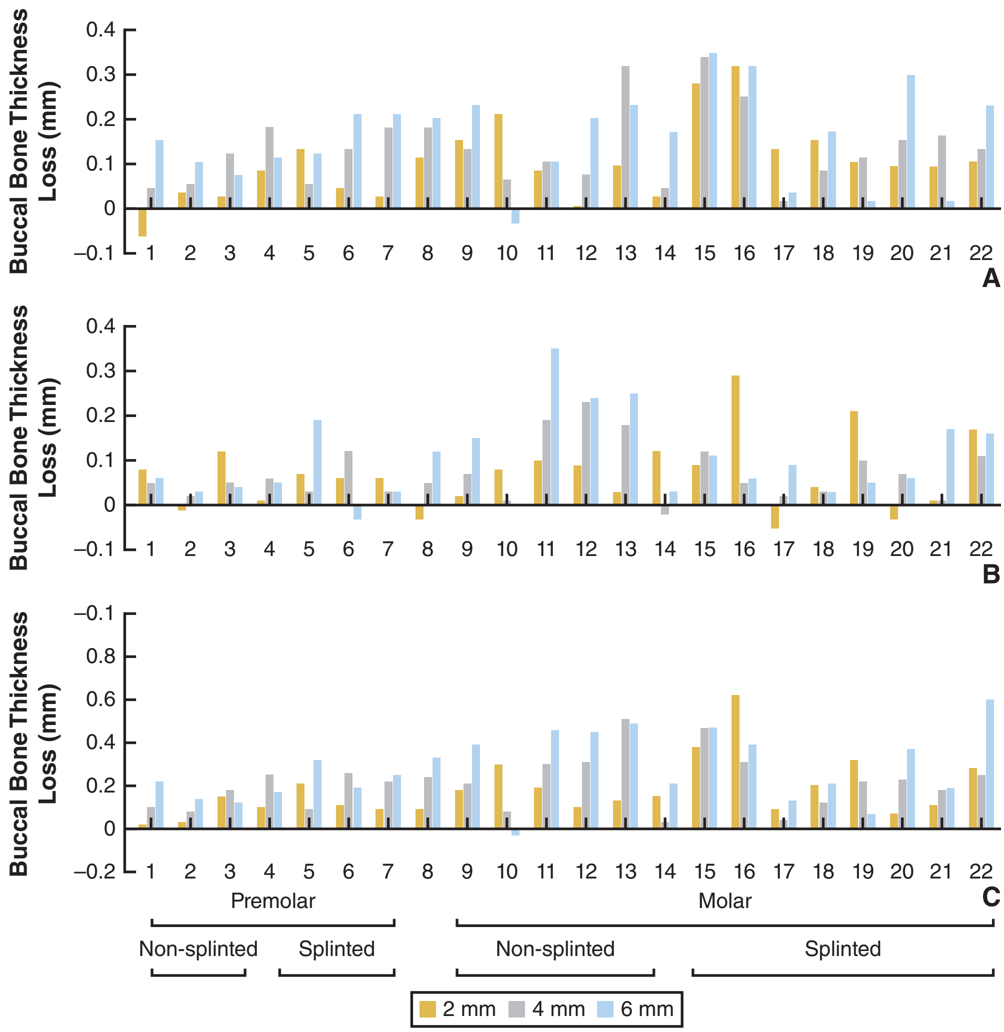

Figure 4. Buccal bone thickness loss at different time intervals (A: 3–15M, B: 15–27M, C: 3–27M) at 3 depth levels (2 mm, 4 mm, 6 mm). M, months after loading.

Figure 7 shows the significant correlation between the SED in the buccal bone area and the change in the buccal bone volume from 3 M to15M (R^2=.57) and 3 M to 27 M (R^2=.67). However, no significant association was observed between the SED and buccal bone changes in the 15 M to 27 M period. No discernible variation was observed between participants treated with a single implant and those treated with a splinted implant.

Figure 8 shows significant relationships between the SED and changes in the BBT at 2 and 4 mm between 3 M and 15 M (2 mm, R^2=.52; 4 mm, R^2=.48) and 3 M and 27 M (2 mm; R^2=.44; 4 mm, R^2=.37). No significant relationship was observed between the SED and changes in the BBT between 15 M and 27 M at all levels.

DISCUSSION

The null hypothesis that the loading forces following superstructure placement would have no impact on peri-implant bone remodeling was rejected. A relationship between mechanical stimuli and bone volume loss and buccal bone thickness loss was found. However, the generalizability of these findings may be limited because of the small sample size. To confirm the results and enhance their accuracy, future studies with larger sample sizes are warranted.

Peri-implant bone remodeling has been extensively studied,[16,21,26,34] and the prevailing consensus suggests that remodeling plays a crucial role in facilitating the proper integration of the implant into the surrounding bone. However, peri-implant bone remodeling can result in bone loss, particularly in the crestal bone region. Bone loss of approximately 1.2 mm reportedly occurs during the first year after implant placement, followed by a subsequent annual bone loss of 0.1 mm.[35] Peri-implant bone remodeling is influenced by factors that include the timing of loading, implant position and dimensions, depth of the implant, and tapering of the

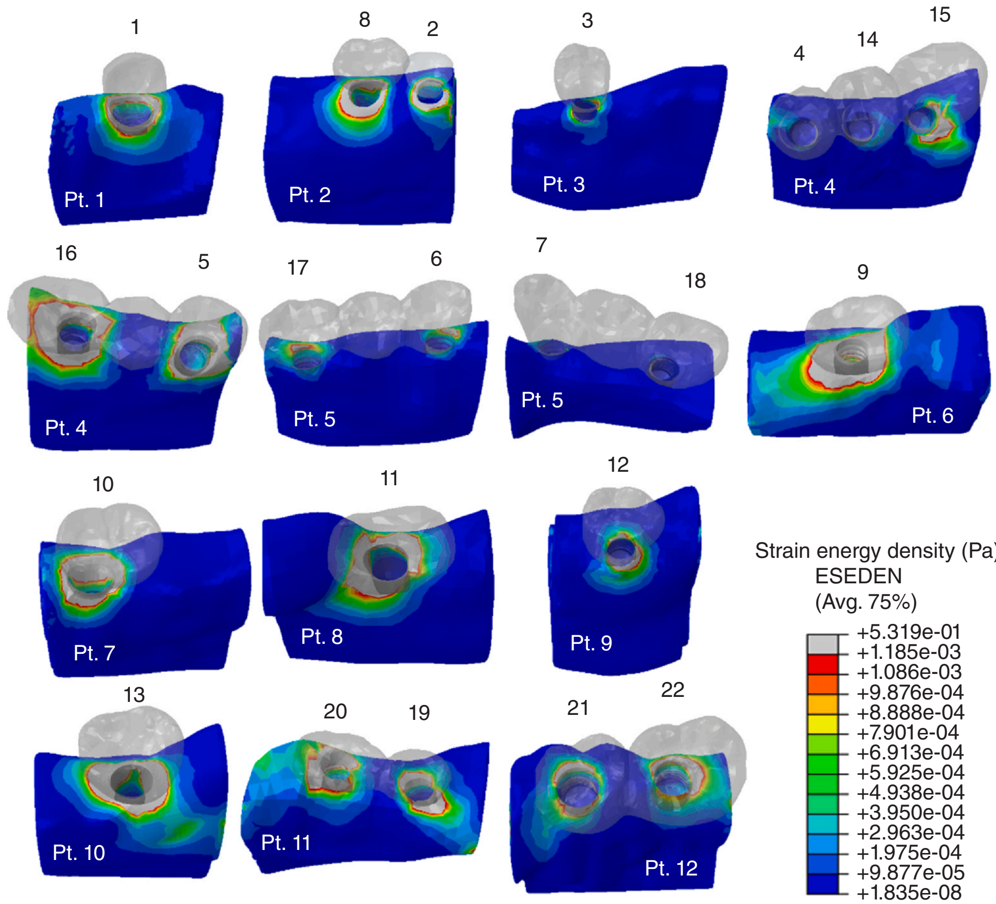

Figure 5. Examples of strain energy density distribution in peri-implant bone in each studied implant. Numbers on figure indicate implant numbers defined in Table 1. Values of strain energy density (Pa) shown in color in bottom right corner.

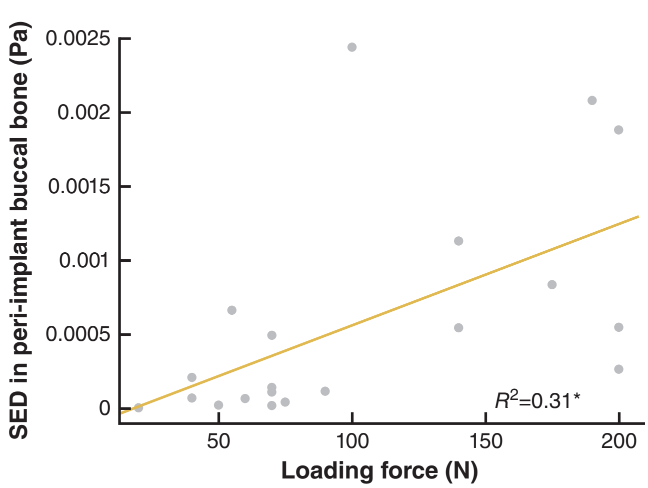

Figure 6. Relationship between strain energy density (SED) in buccal bone area and loading force. Linear regression model of relationship between SED in buccal bone area and loading force. *statistical significance (*P*<.01).

abutment.[6] Bryant and Zarb[36] demonstrated similar peri-implant bone loss in both elderly and young adults; thus, participant age does not significantly contribute to peri-implant bone loss. These findings are consistent with those of the present study. It should be noted that all studied implants demonstrated a favorable outcome with no clinical symptoms and no mucosal recession even in clinical scenarios where bone loss was confirmed. In other words, the horizontal bone resorption observed in this study was at a level that was not clinically problematic.

The integration of real patient data and CBCT images into FEA for dental implant studies presents considerable challenges.[20,22] The conversion of CBCT images into 3D models involves defining the bone surface based on pixel intensity along with manual adjustments by the investigators, which could result in inaccuracies. Therefore, intercalibration of the measurements is necessary. Typically, FEA investigations in dental implantology encompass various components, including the crown, abutment, implant, screw, cement, and even intricate peri-implant bone structures, such as the cortical bone, trabecular bone, and nerve canals.[37] However, certain simplifications were made in the present study. The elements comprising the implant were consolidated into a single component, thus streamlining the

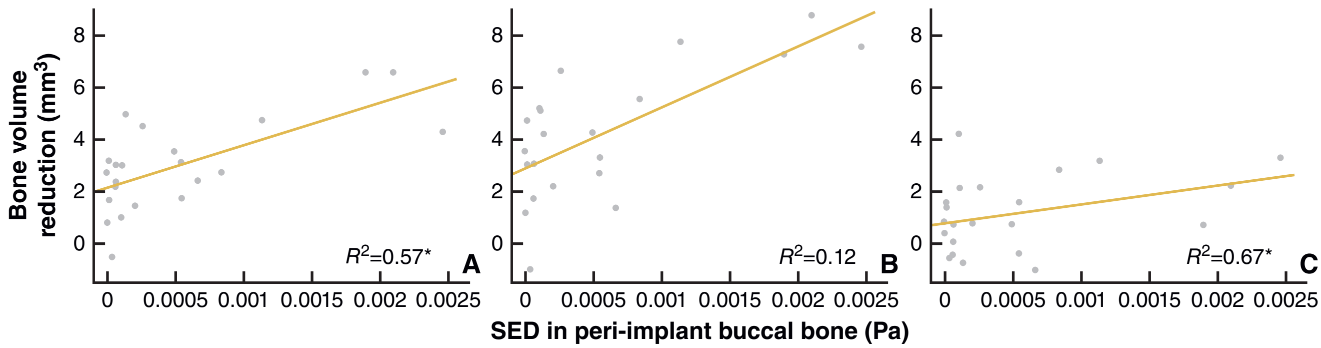

Figure 7. Relationship between strain energy density (SED) in buccal bone area and bone volume loss at different time intervals. A, 3–15M. B, 15–27M. C, 3–27M. M, months after loading. *statistical significance ($P<.01$).

modeling process and permitting a more efficient analysis. Although this approach may overlook the finer nuances and interactions between individual components,[7] it provided a practical solution for generating 22 finite element models, each representing a distinct implant, within the limitations of the study.

Although the Dental Prescale provides valuable data on the occlusal force at clenching, it could not capture

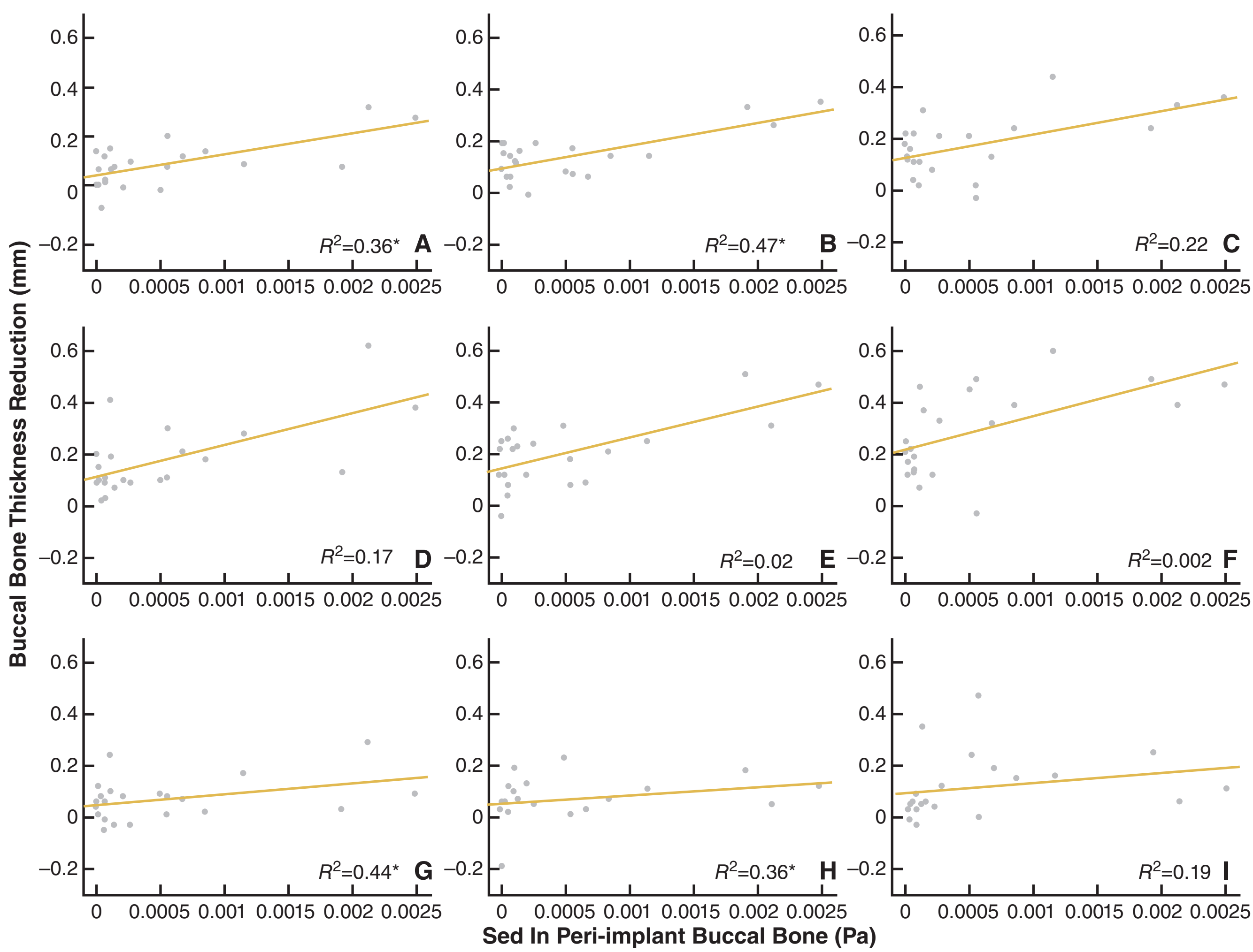

Figure 8. Relationship between strain energy density (SED) in buccal bone area and buccal bone thickness loss at different time intervals and different depths. A, 3–15M at 2 mm from platform. B, 3–15M at 4 mm from platform. C, 3–15M at 6 mm from platform. D, 15–27M at 2 mm. E, 15–27M at 4 mm. F, 15–27M at 6 mm. G, 3–27M at 2 mm. H, 3–27M at 4 mm. I, 3–27M at 6 mm. M, months after loading. *statistical significance ($P<.01$).

the angle at which the occlusal force was exerted. Moreover, the influence of the splinted superstructure on the load on each implant can affect the simulation in peri-implant bone, even though the influence was regarded as small[33] in the present study. To record 3D load dynamics on each implant, more complicated methods of load measurement such as piezoelectric force transducers or strain gauges are needed.[38,39] Consequently, the loading angulation was set perpendicular to the occlusal plane in the analysis, which may not accurately represent the actual forces exerted by the implant in clinical settings. Additionally, the study did not account for any lateral forces exerted by the adjacent teeth, as the measurement method used in the present study did not allow for their assessment.

Both FEA and 3D volumetric analyses aided in quantifying and visualizing time-dependent bone apposition and resorption in terms of morphology, a capability which was lacking in traditional 2-dimensional radiographic image analysis.[26] Accurate visualization and measurement of the actual changes in the peri-implant bone is crucial for studying implant treatment outcomes. The peri-implant buccal bone was chosen as the focal point for investigation in the present study because significant bone remodeling in response to loading primarily occurs on the buccal side as compared with other aspects of the implant.[11] The findings indicated that force applied to the implant was associated with increased bone loss during the first 15 months after loading by regular function. These findings corroborate with those of the existing literature on bone loss attributed to force application.[40–43] Nevertheless, these findings are contradictory to those of Frost,[44] who proposed that the application of suitable loading force would result in remodeling into high-quality bone to accommodate the increased load, a concept that has been supported by recent research.[45,46] The observed change aligns with that of previous studies, highlighting the predominant occurrence of bone changes within approximately the first year after implant placement.[35] Limited evidence exists concerning the specific remodeling process in the subsequent years after superstructure placement.

Recent research has determined that the initial thickness and alterations in the buccal bone can affect the stability of the peri-implant bone after the completion of the healing phase.[47] These findings were consistent with the correlation observed with bone volume. Greater stress on the bone results in increased bone thickness loss, which is attributed to the remodeling process. However, this correlation was not observed during the 15 to 27 months after loading, which was consistent with the aforementioned observations. Nevertheless, the amount of buccal bone volume and thickness loss observed at 15 months was at a clinically acceptable level, and all implants investigated showed favorable clinical outcomes. Inevitable bone resorption caused by implant surgery might be observed, and this can be somewhat facilitated by occlusion.[47]

CONCLUSIONS

Based on the findings of this FEA and clinical study, the following conclusions were drawn:

1. The combined use of FEA in conjunction with clinical data on patient-specific bone morphological changes was useful for predicting the clinical outcomes associated with load-induced bone remodeling.
2. Peri-implant bone changes occurred during the first year after superstructure placement, which may be accelerated by loading.

DATA AVAILABILITY STATEMENT

The data that support the findings of this study are available on request from the corresponding author. The data are not publicly available due to privacy or ethical restrictions.

REFERENCES

1. Albrektsson T, Zarb G, Worthington P, Eriksson AR. The long-term efficacy of currently used dental implants: A review and proposed criteria of success. *Int J Oral Maxillofac Implants*. 1986;1:11–25.
2. Insua A, Monje A, Wang HL, Miron RJ. Basis of Bone metabolism around dental implants during osseointegration and peri-implant bone loss. *J Biomed Mater Res A*. 2017;105:2075–2089.
3. Herrera D, Berglundh T, Schwarz F, et al. Prevention and treatment of peri-implant diseases—The EFP S3 level clinical practice guideline. *J Clin Periodontol*. 2023;50(26):4–76.
4. Qian J, Wennerberg A, Albrektsson T. Reasons for marginal bone loss around oral implants. *Clin Implant Dent Relat Res*. 2012;14:792–807.
5. Pumnil S, Rungsiyakull P, Rungsiyakull C, Elsaka S. Effect of different customized abutment types on stress distribution in implant-supported single crown: A 3D finite element analysis. *J Prosthodont*. 2022;31:e2–e11.
6. Poovarodom P, Rungsiyakull C, Suriyawanakul J, et al. Effect of implant placement depth on bone remodeling in implant-supported single zirconia abutment crowns: A 3D finite element study. *J Prosthodont Res*. 2023;67:278–287.
7. Poovarodom P, Rungsiyakull C, Suriyawanakul J, et al. Effect of gingival height of a titanium base on the biomechanical behavior of 2-piece custom implant abutments: A 3-dimensional nonlinear finite element study. *J Prosthet Dent*. 2023;130:380. .e1–9.
8. Schouten C, Mejier G, Beucken J, et al. The quantitative assessment of peri-implant bone responses using histomorphometry and micro-computed tomography. *Biomaterials*. 2009;30:4539–4549.
9. Stokholm R, Isidor F, Nyengaard J. Histologic and histomorphometric evaluation of peri-implant bone of immediate or delayed occlusal-loaded non-splinted implants in the posterior mandible-an experimental study in monkeys. *Clin Oral Implants Res*. 2014;25:1311–1318.
10. Falcinelli C, Valente F, Vasta M, Traini T. Finite element analysis in implant dentistry: State of the art and future directions. *Dent Mater*. 2023;39:539–556.
11. Trivedi S. Finite element analysis: a boon to dentistry. *J Oral Biol Craniofac Res*. 2014;4:200–203.
12. Meira JB, Jikihara AN, Capetillo P, et al. Finite-element analysis in dentistry. *In: Biomaterial mechanics* 2018:67–89.
13. Wakabayashi N, Ona M, Suzuki T, Igarashi Y. Nonlinear finite element analyses: advances and challenges in dental applications. *J Dent*. 2008;36:463–471.

14. Wada M, Andoh T, Gonda T, Maeda Y. Implant placement with a guided surgery system based on stress analyses utilizing the bone density: A clinical case report. *J Oral Implantol*. 2014;40:603–606.
15. Yang Y, Liu Y, Yuan X, et al. Three-dimensional finite element analysis of stress distribution in short implants with different bone conditions and osseointegration rates. *BMC Oral Health*. 2023;23:220.
16. Kitamura E, Stegaroiu R, Nomura S, Miyakawa O. Biomechanical aspects of marginal bone resorption around osseointegrated implants: considerations based on three-dimensional finite element analysis. *Clin Oral Implants Res*. 2004;15:401–412.
17. Naini RB, Nokar S, Borghei H, Alikhasi M. Tilted or parallel implant placement in the completely edentulous mandible? A three-dimensional finite element analysis. *Int J Oral Maxillofac Implants*. 2011;26:776–781.
18. Tsouknidas A, Giannopoulos D, Savvakis S, et al. The influence of bone quality on the biomechanical behavior of a tooth-implant fixed partial denture: A three-dimensional finite element analysis. *Int J Oral Maxillofac Implants*. 2016;31:e143–e154.
19. Benazzi S, Nguyen HN, Kullmer O, Kupczik K. Dynamic modelling of tooth deformation using occlusal kinematics and finite element analysis. *PLOS ONE*. 2016;11:e0152663.
20. Kang X, Li Y, Wang Y, et al. Relationships of stresses on alveolar bone and abutment of dental implant from various bite forces by three-dimensional finite element analysis. *BioMed Res Int*. 2020;2020:7539628.
21. Sato E, Shigemitsu R, Mito T, et al. The effects of bone remodeling on biomechanical behavior in a patient with an implant-supported overdenture. *Comput Biol Med*. 2021;129:104173.
22. Su K, Zhou Y, Hossaini-Zadeh M, Du J. Effects of implant buccal distance on peri-implant strain: A micro-CT -based finite element analysis. *J Mech Behav Biomed Mater*. 2021;116:104325.
23. Yoda N, Ogawa T, Gunji Y, et al. Effects of food texture on three-dimensional loads on implants during mastication based on in vivo measurements. *Implant Dent*. 2016;25:515–519.
24. Trivedi A, Trivedi S, Narang H, et al. Evaluation of pre and post-loading peri-implant crestal bone levels using cone-beam computed tomography: An in vivo study. *J Contemp Dent Pract*. 2022;23:79–82.
25. Shiga H, Komino M, Uesugi H, et al. Comparison of two dental prescale systems used for the measurement of occlusal force. *Odontology*. 2020;108:676–680.
26. Yoda N, Zheng K, Chen J, et al. Bone morphological effects on post-implantation remodeling of maxillary anterior buccal bone: A clinical and biomechanical study. *J Prosthodont Res*. 2017;61:393–402.
27. Putra RH, Yoda N, Iikubo M, et al. Influence of bone condition on implant placement accuracy with computer-guided surgery. *Int J Implant Dent*. 2020;6:62.
28. Lin D, Li Q, Li W, et al. Mandibular bone remodeling induced by dental implant. *J Biomech*. 2010;43:287–293.
29. Wan B, Chung BH, Zhang MR, et al. The effect of varying occlusal loading conditions on stress distribution in roots of sound and instrumented molar teeth: A finite element analysis. *J Endod*. 2022;48:893–901.
30. Kaleli N, Sarac D, Külünk S, Öztürk Ö. Effect of different restorative crown and customized abutment materials on stress distribution in single implants and peripheral bone: A three-dimensional finite element analysis study. *J Prosthet Dent*. 2018;119:437–445.
31. Leder Horina J, van Rietbergen B, Jurčević Lulić T. Finite element model of load adaptive remodelling induced by orthodontic forces. *Med Eng Phys*. 2018;62:63–68.
32. Su K, Yuan L, Yang J, Du J. Numerical simulation of mandible bone remodeling under tooth loading: A parametric study. *Sci Rep*. 2019;9:14887.
33. Yoda N, Gunji Y, Ogawa T, et al. In vivo load measurement for evaluating the splinting effects of implant-supported superstructures: A pilot study. *Int J Prosthodont*. 2013;26:143–146.
34. Albrektsson T, Dahlin C, Jemt T, et al. Is marginal bone loss around oral implants the result of a provoked foreign body reaction? *Clin Implant Dent Relat Res*. 2014;16:155–165.
35. Adell R, Lekholm U, Rockler B, Brånemark PI. A 15-year study of osseointegrated implants in the treatment of the edentulous jaw. *Int J Oral Surg*. 1981;10:387–416.
36. Bryant SR, Zarb GA. Crestal bone loss proximal to oral implants in older and younger adults. *J Prosthet Dent*. 2003;89:589–597.
37. Hosseini-Faradonbeh SA, Katoozian HR. Biomechanical evaluation of the long-term stability of dental implant using finite element modeling method: A systematic review. *J Adv Prosthodont*. 2022;14:182–202.
38. Röhrle O, Saini H, Ackland DC. Occlusal loading during biting from an experimental and simulation point of view. *Dent Mater*. 2018;34:58–68.
39. Assoratgoon I, Yoda N, Iwamoto M, et al. In vivo measurement of three-dimensional load exerted on dental implants: A literature review. *Int J Implant Dent*. 2022;8:52.
40. Akca K, Cehreli MC. Biomechanical consequences of progressive marginal bone loss around oral implants: A finite element stress analysis. *Med Biol Eng Comput*. 2006;44:527–535.
41. Al-Shabeeb MS, Al-Askar M, Al-Rasheed A, et al. Alveolar bone remodeling around immediate implants placed in accordance with the extraction socket classification: A three-dimensional microcomputed tomography analysis. *J Periodontol*. 2012;83:981–987.
42. Pérez-Pevida E, Chávarri-Prado D, Diéguez-Pereira M, et al. Consequences of peri-implant bone loss in the occlusal load transfer to the supporting bone in terms of magnitude of stress, strain, and stress distribution: A finite element analysis. *BioMed Res Int*. 2021;2021:3087071.
43. Bredberg C, Vu C, Häggman-Henrikson B, Chrcanovic BR. Marginal bone loss around dental implants: comparison between matched groups of bruxers and non-bruxers: A retrospective case–control study. *Clin Implant Dent Relat Res*. 2023;25:124–132.
44. Frost HM. Suggested fundamental concepts in skeletal physiology. *Calcif Tissue Int*. 1993;52:1–4.
45. Okawara H, Arai Y, Matsuno H, et al. Effect of load-induced local mechanical strain on peri-implant bone cell activity related to bone resorption and formation in mice: An analysis of histology and strain distributions. *J Mech Behav Biomed Mater*. 2021;116:104370.
46. Tian Y, Sadowsky SJ, Brunski JB, et al. Effects of masticatory loading on bone remodeling around teeth versus implants: Insights from a preclinical model. *Clin Oral Implants Res*. 2022;33:342–352.
47. Monje A, Roccuzzo A, Buser D, Wang HL. Significance of buccal bone wall thickness in the fate of peri-implant hard and soft tissues: A systematic review. *Clin Oral Implants Res*. 2023;34:157–176.

Corresponding author:
Dr Nobuhiro Yoda
Division of Advanced Prosthetic Dentistry
Tohoku University Graduate School of Dentistry
4–1, Seiryo-machi
Aoba-ku, Sendai 980–8575
JAPAN
Email: nobuhiro.yoda.e2@tohoku.ac.jp

CRediT authorship contribution statement

Itt Assoratgoon: Conceptualization, Data curation and investigation, Methodology, Formal analysis, Writing – original draft preparation, Visualization. **Boyang Wan**: Data curation and investigation, Methodology, Formal analysis, Writing – original draft preparation, Visualization. **Taichi Tenkumo**: Data curation and investigation, Writing – review and editing. **Tomoya Sato**: Data curation and investigation, Methodology, Funding acquisition. **Tetsuo Kawata**: Data curation and investigation, Methodology, Funding acquisition. **Ramadhan Hardani Putra**: Methodology, Writing – review and editing. **Chi Wu**: Methodology, Writing – review and editing. **Hiroshi Egusa**: Conceptualization, Writing – review and editing. **Qing Li**: Conceptualization, Methodology, Writing – review and editing. **Keiichi Sasaki**: Conceptualization, Writing – review and editing. **Yoda Nobuhiro**: Conceptualization, Data curation and investigation, Methodology, Formal analysis, Writing – review and editing, Visualization.

https://doi.org/10.1016/j.prosdent.2025.01.015